Contemporary Synthesis of Ultrasmall (sub-10 nm) Upconverting Nanomaterials

Tanmaya Joshi,* Constantin Mamat, and Holger Stephan*[a]

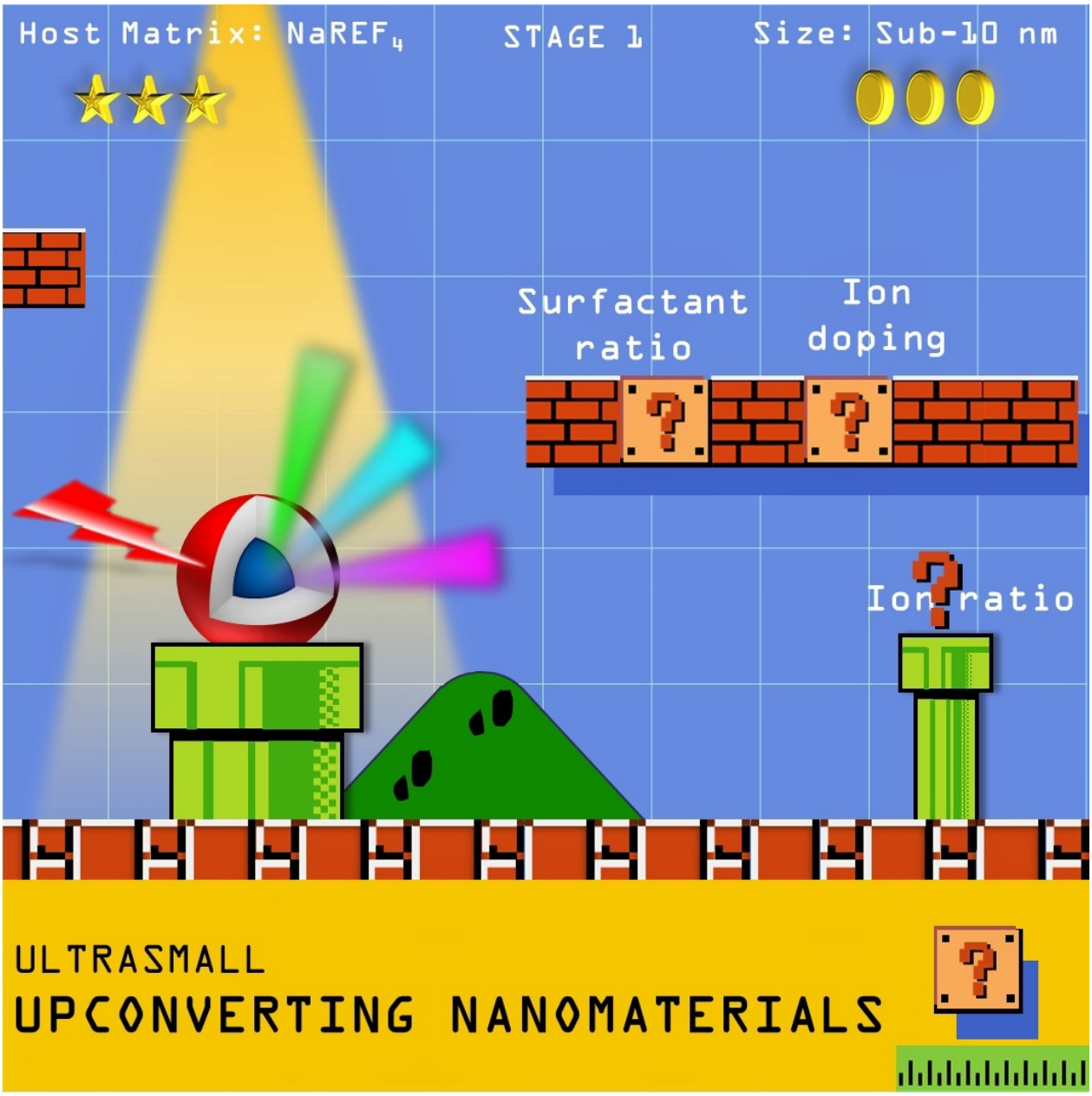

Due to their unique photophysical properties, upconverting nanoparticles (UCNPs), i.e. particles capable of converting near-infrared (NIR) photons into tunable emissions in the range of ultraviolet (UV) to NIR, have great potential for use in various biomedical fields such as bioimaging, photodynamic therapy and bioanalytical applications. As far as biomedical applications are concerned, these materials have a number of advantageous properties such as brilliant luminescence and exceptional photostability. Very small "stealth" particles (sub-10 nm), which can circulate in the body largely undetected by the immune system, are particularly important for in vivo use. The fabrication of such particles, which simultaneously have a defined (ultrasmall) size and the required optical properties, is a great challenge and an area that is in its infancy. This minireview provides a concise overview of recent developments on appropriate synthetic methodologies to produce such UCNPs. Particular attention was given to the influence of both surfactants and dopants used to precisely adjust size, crystalline phase and optical properties of UCNPs.

1. Introduction

The translation of nanomaterials (NMs) from laboratory to clinical and industrial applications strongly relies on the availability of synthetic methods that allow scalable production of NMs. Devising such methods is, however, anything but routine because it also a key requirement that such methods do offer a precise control of shape, size, phase and stoichiometric elemental composition in order to produce NMs possessing similar physical and optical properties. This limits the choice of employable methodologies, especially when aiming to develop NMs for applications that require the materials to possess very specific features.

Lanthanide-doped upconversion nanoparticles (UCNPs) are one such upcoming class of NMs that require a proper management of physical and optical properties in order to exploit them for biomedical applications.[1–5] Their unique anti-Stokes optical property offers significant advantages over conventional photoluminescent materials used as bioimaging probes.[3,6–12] Excitement around UCNPs also stems from the feasibility to use near-infrared (NIR) light for their excitation, which yields high photochemical stability and reduced autofluorescence interference. Interest also comes from their other exploitable properties for rapid multiplexed analyses, such as tunable emission wavelengths, large anti-Stokes shifts, and long emission lifetimes.[13–15] While the concept of energy transfer in UCNPs is reasonably well established,[16–18] the knowledge on how to create ultrasmall (sub-10 nm) but bright NIR-to-UV UCNPs is still lacking.[4,19–20] This review aims to shed light on the existing methods that may help in overcoming this size-related roadblock to their biologically important applications. In other words, this minireview highlights the current state-of-the-art in the synthesis of sub-10 nm UCNPs, mainly focussing on direct pathways to produce materials below this size threshold. It should be noted that the strategies discussed herein mostly produce hydrophobic materials and further surface modification is indeed required for them to be deployable in a biological environment. These modification strategies have not been included within the scope of this minireview, and the interested readers are directed to other good reviews covering these and other pertinent aspects related to the applications of UCNPs.[6,12,14,16,21–33]

[a] Dr. T. Joshi, Dr. C. Mamat, Dr. H. Stephan
Institute of Radiopharmaceutical Cancer Research
Helmholtz-Zentrum Dresden-Rossendorf
Bautzner Landstraße 400, D 01328 Dresden, Germany
E-mail: t.joshi@hzdr.de
h.stephan@hzdr.de

2. UCNPs – Composition Considerations

UCNPs can exist in two polymorphs: cubic (α-phase – a metastable high-temperature phase) and hexagonal (β-phase – a thermodynamically stable low-temperature phase). A transformation from α- to the β-phase can be achieved via careful manipulation of the reaction time or temperature used for the synthesis. The efficiency of UC luminescence is approximately one order of magnitude higher for β-phase nanocrystals in comparison to the α-phase NMs.[34] Typically, the UCNPs are composed of lanthanide (Ln^{3+}) ions doped in an optically inert fluoride-based host matrix, which commonly comprises of rare-earth salts ($NaREF_4$, RE = Y, Gd, Lu). A key to designing UCNPs with tuned emission profile is to dope them with an appropriate sensitiser/activator Ln^{3+} ion pair that later allows the desired transfer of excitation energy to happen within the nanocrystal. For this, Yb^{3+} or Nd^{3+} are used as sensitiser ions, whereas the choice for activator ions may vary depending on the UV/blue, green and/or red emission output wanted for a particular application (Table 1).[16,35–36] Besides the crystallite phase, additional factors such as the host material, crystallite

Table 1. Typical lanthanide ion emissions used for multicolour tuning of UCNPs.[16,35]

Activator	UC emission[a] (nm)
Pr^{3+}	485(s), 520(w), 538(w), 605(s), 635(w), 645(s), 670(w), 690(w), 720(w)
Nd^{3+}	430(w), 482(w), 525(s), 535(s), 600(s), 664(s), 766(s)
Sm^{3+}	555(s), 590(s)
Eu^{3+}	590(s), 613(s), 690(w)
Gd^{3+}	204(w), 254(w), 278(m), 305(w), 312(s)
Tb^{3+}	489(w), 541(s), 584(w), 619(w)
Dy^{3+}	570(s)
Ho^{3+}	542(s), 655(w)
Er^{3+}	525(m), 542(s), 655(s)
Tm^{3+}	362(w), 450(w), 475(s), 644(w), 694(w), 800(s)

[a] emission intensities are given as strong (s), medium (m), and weak (w).

size and the concentration of dopant ions can have a large impact on the optical properties of such materials. A number of good reviews have covered in detail the influential role of these factors as well as the different strategies for UC emission tuning in lanthanide-doped NMs.[7,16,35,37–40]

2.1. UCNPs – Size Considerations for Biological Applications

NP size can influence their blood circulation lifetime, ultimately affecting the distribution and clearance from the body.[32,41–44] The key point to avoid when developing UCNPs for bioapplications is their accumulation in liver and spleen. In this connection, increasing interest has been in keeping the size of UCNPs below the required threshold for renal clearance.[32,41–44] Generally, NPs with hydrodynamic diameter below 5.5 nm can easily pass through the glomeruli for their excretion through urine.[45–46]

In biological fluid, the NPs can have a tendency to interact with proteins, phospholipids and other biomolecules.[33,41–43,47–48] This NP-biomolecule interaction is generally unspecific and can add considerably to the overall size of the NPs in vivo. The challenge of controlling and/or accurately forecasting the extent of such interaction has been met with limited success.[28,33,41–43,49–52] Moreover, as the size of UCNPs becomes smaller, their luminescence intensity also decreases.[4,53] As a result, it becomes necessary to put forward a synergistic combination of strategies that enable size regulation in UCNPs while minimising the consequential loss in UC emission.[54–55] Otherwise, it could render the produced UCNPs unsuitable for bioimaging applications. One of the main problems in this connection is that although many proof-of-concept strategies exist for improving the optical properties of UCNPs, very less work has been done to link these with UCNPs that are below 10 nm in size. In fact, producing ultrasmall (sub-10 nm) UCNPs with optical properties appropriately tailored for biomedical applications continues to be one of the biggest challenges in the field.[4,10,44,55–57] Thus, herein we provide a very concise overview of the existing studies dealing with the production of such ultrasmall UCNPs.

2.2. UCNPs – Synthetic Methodologies

UCNPs are most commonly synthesised by using hydrothermal synthesis, thermal decomposition or co-precipitation procedures.[36,40,58–60] Hydrothermal method, a continuous bottom-up approach, has been employed for the synthesis of both α-phase and β-phase UCNPs. In a typical procedure, the lanthanide salts (e.g. as chlorides, nitrates, or oxides), fluoride precursors, solvents (e.g. water, ethanol, or acetic acid) and certain complexants/surfactants such as ethylenediaminetetraacetic acid, cetyltrimethylammonium bromide are heated above the critical point of the solvent. However, the heating is conducted in a sealed reaction environment by using autoclaves, which makes it extremely complex to observe the nanocrystal growth during the synthesis. An alternative synthetic strategy is the thermal decomposition of Ln^{3+} trifluoroacetates in high boiling solvents such as octadecene (ODE), with surfactants such as oleic acid (OA), oleylamine (OM) or trioctylphosphine oxide (TOPO) at ~310–320 °C. During the synthesis, nucleation of lanthanide fluorides takes place, followed by the growth of nuclei into nanocrystals. This method allows for the production of high quality UCNPs with narrow size distributions, and with good size control in a relatively short time. However, the drawbacks of this procedure include the toxicity and air-sensitivity of the metal precursors. This method produces hydrophobic UCNPs and further surface modification is always required in order to obtain water dispersible NPs for biological applications. The most convenient and straightforward method for elaborating UCNPs is co-precipitation, which has been used by several groups to deliver 3–30 nm size NPs, with a narrow size distribution.[11,20,27,58,61–63] Here, the synthesis is performed using a non-coordinating high boiling solvent such as ODE with, typically, OA as the surface ligand. Lanthanides are added as chloride salts, and heated to 120–160 °C to generate $Ln(oleate)_3$ in situ. Then, sodium hydroxide (NaOH) and ammonium fluoride (NH_4F) are added as source of Na^+ and F^- ions, respectively, before a second heating step to 300–325 °C. After cooling, the oleate-coated UCNPs are isolated via centrifugation. This method offers easy crystal phase and size control, and is more cost-effective because the used Ln^{3+} precursors are less expensive than the

Tanmaya Joshi obtained his PhD (2012) from Monash University with Prof. Leone Spiccia. Since Nov. 2016, he is at the Institute of Radiopharmaceutical Cancer Research, Helmholtz-Zentrum Dresden-Rossendorf (HZDR), first as an Alexander von Humboldt fellow, and then since 2019, as HZDR High Potential Fellow. One of his current research focus is the biocompatibilisation of ultrasmall nanomaterials for their later development as new imaging, therapeutic and diagnostic agents.

Holger Stephan studied chemistry and received his PhD degree from the Bergakademie Freiberg in 1989. Since 1998, he has been working at the Helmholtz-Zentrum Dresden Rossendorf, where he is currently leading the research group "Nanoscalic Systems" group at the Institute of Radiopharmaceutical Cancer Research. His research focuses on the development of radiometal complexes, including radiolabelled "stealth" nanoparticles for therapeutic and diagnostic applications. Multinuclear particles (polyoxometalates, rhenium clusters, silicon quantum dots, upconverting nanomaterials) with antitumour activity, photosensitising and radiation sensitising properties are of special interest.

Table 2. Representative examples for contributions made towards the synthesis of sub-10 nm UCNPs with focus on the influence of surfactants and dopants.

Category	Host:dopant	Solvent	Temperature [°C]	Size [nm]	Phase	Ref.
Surfactant ratio	$NaYF_4$:Yb^{3+},Er^{3+}	OM/OA	285	7.0	α	67
	$NaYF_4$:Yb^{3+},Tm^{3+}	OM/OA	275	~7.0	α	68
	$NaYbF_4$:Tm^{3+},Lu^{3+}	OM/OA/ODE	320	7.2	β	69
	$NaYF_4$:Yb^{3+},Er^{3+}	OM/OA/ODE	310	5.4	β	70
	$NaYF_4$:Nd^{3+},Yb^{3+},Er^{3+}	T66/OA	319	9.0	β	72
Ion ratio	$NaYF_4$:Yb^{3+},Er^{3+}	OA/ODE	300	5.3	β	74,75
	$NaYF_4$:Yb^{3+},Er^{3+}	OA/ODE	300	3–4	α	75
	$NaYbF_4$:Tm^{3+}	OA/ODE	320	7–10	β	76
	$NaYF_4$:Yb^{3+},Er^{3+}	OM/OA/ODE	300	5.4	β	78
Ion doping	$NaYF_4$:Yb^{3+},Er^{3+},Gd^{3+}	OA/ODE	230	10.0	β	79
	$NaLuF_4$:Gd^{3+},Yb^{3+},Tm^{3+}	OM	340	7.8	β	81
	$NaYbF_4$:Tm^{3+},Gd^{3+}	OA/ODE	300	7–15	β	82
	$KGdF_4$:Tm^{3+},Yb^{3+}	OA/ODE	300	3.7	β	83
	$NaLuF_4$:Gd^{3+},Yb^{3+},Er^{3+}	OA/ODE	300	4.4	α	84
	$NaYF_4$:Gd^{3+},Yb^{3+},Er^{3+}	OA/ODE	300	3.8	β	84
	$NaGdF_4$:Yb^{3+},Tm^{3+},Nd^{3+},Ca^{2+}	OA/ODE	300	7.7–9.3	β	85

corresponding trifluoroacetates. Due to the high reaction temperature and the sensitivity of NPs towards oxygen impurities, control over reaction parameters must be precise in order to produce UCNPs with narrow size distributions. Factors such as pressure, rate of heating and cooling, and reaction time also play an important role in the crystalline size and morphology of the material produced. As for the thermal decomposition method, further surface modification of UCNPs produced using this method is necessary for them to be rendered hydrophilic. Beyond these methods, the preparation of Ln^{3+}-doped UCNPs with different sizes, shape and optical features has been explored via other approaches such as, ionic-liquid-based synthesis, microwave-assisted, and microemulsion-based synthesis. For deeper understanding, the interested readers are advised to refer to the many excellent reviews covering each of these methods for controlled synthesis of UCNPs.[23,36,40,64]

2.3. Sub-10 nm UCNPs

2.3.1. Surfactant Ratio

Preparation of UCNPs has been explored with a variety of host matrices, such as, fluorides, oxides, sulphides, phosphates, and vanadates.[25,36,65] In this review, we discuss only the representative examples from synthesis' involving fluoride-based host matrix (Table 2). The fluorides, which exhibit low phonon energy of ~4.19 kJ/mol, high chemical and thermal stability, produce superior UC features making them an ideal host choice in synthesis of UCNPs.[58] The fluoride ion source in all of the reported preparation methodologies are usually the respective trifluoroacetate salts of the lanthanides or inorganic fluorides (e.g., NaF, NH_4F). Likewise, each of these reactions employ an appropriate surfactant for which the choice may vary depending on the synthetic methodology selected.

High boiling organic solvents such as OA, OM and ODE play a critical role in synthesis of sub-10 nm UCNPs. Solvent ratios in the reaction mixture have shown to influence the size and phase of the final NPs. A body of work has been done towards understanding the cooperative effect different solvents can have on the size of produced NPs.[26,58,61–62,66] For example, through systematic IR and NMR studies, Niu et al. have shown that controlling the concentration of *N*-octadecyloleamide (OOA), formed from amidation reaction between OA and OM at elevated temperatures employed for thermolysis ($\geq$250 °C), can assist in reducing the size of $NaYF_4$: 20% Yb^{3+}, 2% Er^{3+} UCNPs.[67] As surfactant, OOA shows a much higher affinity for NPs. The authors noted a decrease in particle size as the ratio of OM/OA was increased (Figure 1).[67] In this synthesis, α-phase $NaYF_4$ NPs with crystallite size of 7.0 nm were obtained by carrying out the reaction in OM only, at 285 °C over a period of

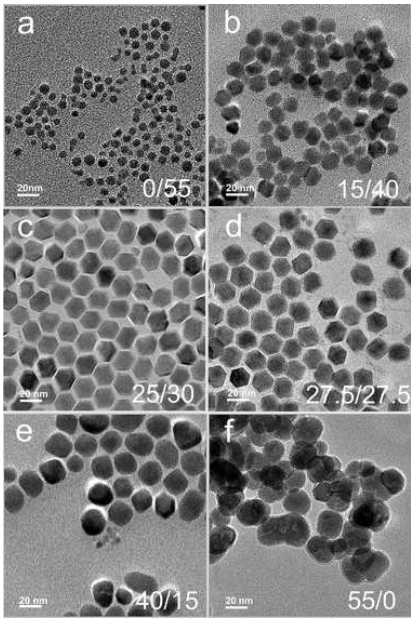

Figure 1. TEM images of $NaYF_4$: 20% Yb^{3+}, 2% Er^{3+} UCNPs prepared with a OA/OM ratio of a) 0/55, b) 15/40, c) 25/30, d) 27.5/27.5, e) 40/15, f) 55/0. Adapted with permission from ref. [67]. Copyright 2011 Royal Society of Chemistry.

1 h. The authors reported similar findings for $NaGdF_4$: 20% Yb^{3+}, 2% Er^{3+} UCNPs.[67]

Prasad and coworkers reported another synthetic methodology for obtaining ultrasmall photoluminescent $NaYF_4$: 2–100% Yb^{3+}, 2% Tm^{3+} nanocrystals with particle sizes ca. 7 nm, albeit in cubic phase.[68] Once again, a mixture of OA/OM in the ratio 2:1 (v/v) was deployed with thermal decomposition at 275 °C for 1 h (Figure 2). The authors noted a 43-fold increase in NIR UC as Yb^{3+} content was increased to 100% for the $NaYbF_4$:2% Tm^{3+} UCNPs, with no significant changes in particle size.[68]

Qin and co-workers also observed a similar effect of the OM/OA ratio on the size of UCNPs, and of the Yb^{3+} content on their UC emission.[69] They synthesized 7.2 nm hexagonal β-phase $NaTm_{0.02}Lu_{0.98-x}Yb_xF_4$ particles by using OM/OA in the ratio 1.25:1 (v/v) at 320 °C for 1 h. In this case, the phase transformation from cubic to hexagonal was attributed to the elevation in reaction temperature.[69] The study also marked the β-$NaYbF_4$-based UCNPs as the best host for ultraviolet UC via Tm^{3+} doping. In another approach, Cohen and coworkers were able to establish a synthetic control over the formation of sub-10 nm pure β-$NaYF_4$ UCNPs by using a two-step thermal decomposition method.[70] Particles with both core and core/shell architecture were prepared from rare-earth chloride salts, sodium oleate (Na-OA), OM and NH_4F in OA and ODE.[70] They optimized the OM concentration (0–1.12 M), Y^{3+}/F^- ratio (1:4–1:8), reaction temperature (290–325 °C) and time (15–60 min) to produce monodispersed particles as small as 5 nm in size (Table 3), which exhibited optical features comparable to the other larger sized UCNPs (≥25 nm). These particles could be excited at 980 nm with visible region UC and showed no blinking or photobleaching (Figure 3).[70]

Previous works have largely concentrated on using high-boiling solvents such as OM or trioctylphosphine oxide (TOPO) for the synthesis of UCNPs.[36,71] Moving away from these, Hesse et al. developed a co-precipitation method using Therminol® 66 (T66), a commercially available fluid composed of a mixture of ter- and polyphenyls, as reaction co-solvent.[72] The authors showed that it was possible to control the crystal phase of the synthesised NPs by exercising strict control over the ratio of T66:OA used (Table 4). In neat T66, the $NaYF_4$ UCNPs were obtained in cubic phase, whereas the reaction in T66:OA (3:2 v/v) resulted in pure hexagonal phase NPs. Importantly, this method requires very short reaction time of 10 min at 319 °C for producing particles that are sub-10 nm in size.[72]

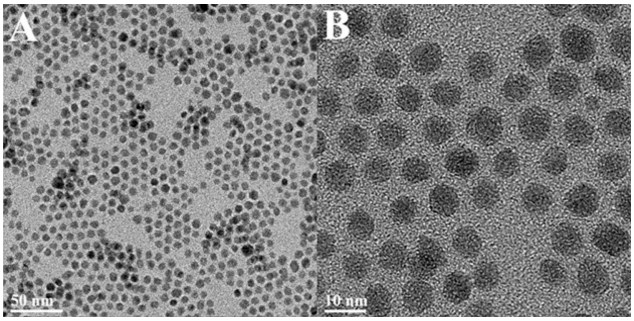

Figure 2. TEM images of cubic phase $NaYF_4$: 2% Tm^{3+}, 20% Yb^{3+} UCNPs obtained with an average diameter ca. 7.1 nm by using OA/OM in 2/1 ratio. Adapted with permission from ref. [68]. Copyright 2010 American Chemical Society.

Table 3. Optimised reaction conditions for the synthesis of sub-10 nm β-$NaYF_4$: 20% Yb^{3+}, 2% Er^{3+} nanocrystals.[70]

Diameter (nm)	Temperature [°C]	[OM] [M]	Time [min]
5.4	310	1.12	45
6.5	310	0.75	45
7.0	318	0.75	45
8.1	320	0.75	45

2.3.2. Ion Ratio and Ion Doping

The molar ratios of sodium, fluoride and rare-earth ions used in the synthesis can affect the growth of UCNPs and the efficiency of UC luminescence.[54] For example, Haase and coworkers showed that by varying the ratio of sodium to gadolinium ions, it was possible to produce β-$NaGdF_4$ particles between sizes of 4–60 nm.[73] Here, the formation of β-phase particles was facilitated by Ostwald-ripening of ~4 nm α-phase NPs, upon heating in OA/ODE. Interestingly, the ratio of sodium to gadolinium ions used for the preparation of α-phase precursor material governed the final size of the NPs. Through systematic studies, the researchers concluded that the growth behaviour of both α- and β-phase UCNPs is significantly sensitive to the

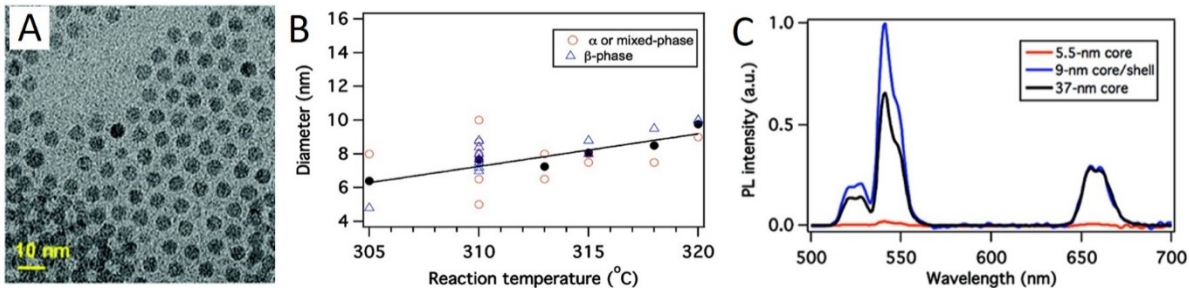

Figure 3. (A) TEM images of 5 nm size β-$NaYF_4$: 20% Yb^{3+}, 2% Er^{3+} UCNPs. (B) The temperature dependent growth of UCNPs prepared using 0.75 M oleylamine (reaction time = 45 min). (C) Resultant UC emission spectra of the UCNPs (in hexane) upon excitation at λ = 980 nm.[70] Adapted with permission from ref. [70]. Copyright 2012 American Chemical Society.

Table 4. $NaYF_4$-based UCNPs synthesised using Therminol® 66 (T66) as co-solvent.[72]

Sample	Composition	T66/OA (v/v)	Time [min]	Temperature [°C]	Phase
A	$NaYF_4$: $Nd^{3+}/Yb^{3+}/Er^{3+}$ (1/20/2%): core	3:2	10	319	β
B	$NaYF_4$: $Nd^{3+}/Yb^{3+}/Er^{3+}$ (1/20/2%): core	3:2	60	320	β
	$NaYF_4$: Nd^{3+}/Yb^{3+} (25/10%): shell		5	305	β
C	$NaYF_4$: $Nd^{3+}/Yb^{3+}/Er^{3+}$ (1/20/2%): core	3:2	10	319	β
	$NaYF_4$: Nd^{3+}/Yb^{3+} (25/10%): shell		5	305	β
D	$NaYF_4$: $Nd^{3+}/Yb^{3+}/Er^{3+}$ (1/20/2%): core	3:0	10	303	α
E	$NaYF_4$: Yb^{3+}/Er^{3+} (20/2%): core	3:2	10	319	β

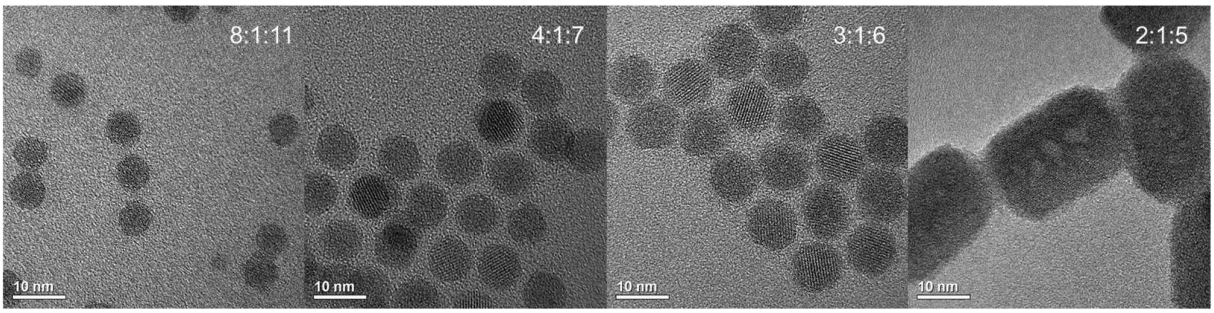

Figure 4. The growth behavior of β-$NaYF_4$:Yb^{3+},Er^{3+} UCNPs prepared by Ostwald ripening of sub-10 nm α-$NaYF_4$:Yb^{3+},Er^{3+} NPs, upon heating in OA/ODE at 300 °C with varying amounts of Na-OA, RE-OA and NH_4F (used molar ratio given in the TEM image). Adapted with permission from ref [74]. Copyright 2014 Royal Society of Chemistry.

amount of sodium ion (in form of sodium oleate) employed in the particle synthesis.[74–75] Monodispersed β-$NaYF_4$:Yb^{3+},Er^{3+} UCNPs with core size as low as 5 nm could be prepared in gram-scale by using Na/Y ratio of 8:1, heating the reaction components in OA/ODE at 300 °C (Figure 4).[74]

In contrast, the α-$NaYF_4$ particles of 3–4 nm in diameter could be prepared by lowering the sodium to yttrium content to 2:1.[75] The authors extended this work to synthesise the β-phase core/shell (c/s) UCNPs, also below 10 nm in size (Figure 5).[75] Interestingly, this preparation required no additional co-doping as the extent of shell growth on the surface of core material was controlled by the dissolution reactivity of α-phase precursor in the presence of the β-phase core particles, both prepared from a different Na/Y ratio.[75]

Huang and coworkers also reported a one-pot thermal coprecipitation methodology that could yield β-$NaYbF_4$ particles as small as 7 nm in size.[76] They noted that the concentration of F^- ions in the reaction mixture had a significant influence on the growth size of the UCNPs, with higher amount of F^- (as NH_4F) favouring the formation of smaller sized particles (Figure 6).[76] In principle, their method can also be extended to the preparation of hexagonal phase sub-10 nm size particles for other group III β-$NaLnF_4$ materials (Ln = Ho, Er, Tm, Lu), ways for which are otherwise very limited.[58,75,77]

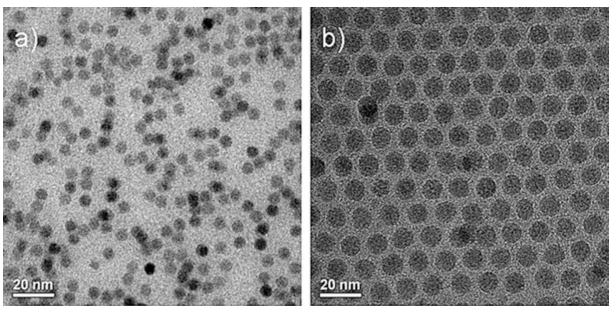

Figure 5. TEM images of sub-10 nm β-$NaYF_4$ core and core/shell particles obtained by Haase and coworkers from the heating of α-phase precursors. Adapted with permission from ref. [75]. Copyright 2016 John Wiley and Sons.

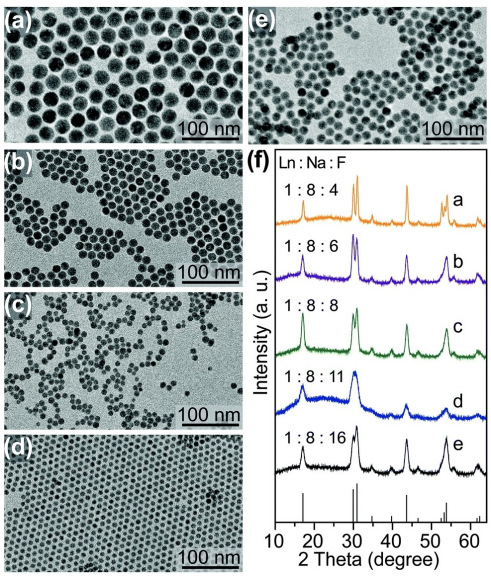

Figure 6. TEM images of Tm^{3+} containing $NaYbF_4$ UCNPs prepared using $Ln^{3+}/Na^+/F^-$ molar ratio of a) 1/8/4, b) 1/8/6, c) 1/8/8, d) 1/8/11, e) 1/8/16, and f) X-ray powder diffractograms of the synthesised UCNPs. Adapted with permission from ref. [76]. Copyright 2017 American Chemical Society.

Li et al. also confirmed that the fluoride concentration plays a crucial role in limiting the crystal size of β-$NaLnF_4$ UCNPs.[78] For size tuning of β-$NaYF_4$:Yb^{3+},Er^{3+}, the authors evaluated different molar ratios of $Na^+/Ln^{3+}/F^-$, as well as the reaction temperature. They prepared sub-10 nm β-$NaYF_4$:Yb^{3+},Er^{3+} core (Figure 7) and β-$NaYF_4$:Yb^{3+},Er^{3+}@$NaLnF_4$ (Ln = Y^{3+}, Gd^{3+}, Lu^{3+}) core/shell UCNPs by carrying out the co-precipitation process, with strictly defined Na-OA and NH_4F concentration, at 300 °C.[78] The core/shell UCNPs were formed with a particle size of ~9 nm, and showed up to 85-fold enhancement in luminescence intensity.[78]

In recent years, substituting the Ln^{3+} in the host matrix with small amounts of lanthanide ions with larger ionic radii has become another effective way for reducing the size of β-$NaYF_4$ UCNPs.[58,79–80] The key advantage here is that it is a single variable control (dopant ion concentration) strategy, as against the other synthesis approaches that require multivariable control to achieve size tuning. For example, Wang et al. found that by intentionally doping Gd^{3+} ions in the $NaYF_4$-based crystal lattice, the size of the resulting particles can be brought down to sub-10 nm range.[79] The authors noted that the Gd^{3+} doping also has a strong influence on the particle phase and reaction temperature, yielding monodispersed hexagonal phase NPs at a lowered temperature of 230 °C.[79] Li and co-workers also adopted a similar approach for preparing sub-10 nm β-$NaLuF_4$ UCNPs.[81] The particles doped with Gd^{3+} (24 mol%), Yb^{3+} (20 mol%) and Tm^{3+} (1 mol%) were synthesised by thermal decomposition in OM, and showed a size of 7.8 nm by TEM. In addition, the authors showed that the particles can be easily rendered hydrophilic by exchanging the surface ligands with citric acid without compromising their hydrodynamic size (~10 nm), and have highly intense UC luminescence upon excitation at λ = 980 nm, marking their suitability for in vivo bioimaging.[81] That the Gd^{3+} ions when doped in appropriate concentration can help to control the phase and size of the UCNPs has also been shown by Prasad and coworkers.[82] In this case, the authors used Gd^{3+} doping for preparing small-sized NIR-to-NIR upconverting $NaYbF_4$ nanospheres and nanoplates, which were both monodispersed and hexagonal. The authors proposed that the Gd^{3+} doping facilitates the α→β phase transformation by lowering the energy barrier for such transition (Figure 8).[82]

Another good example of Gd^{3+} doped NIR-to-NIR upconverting ultrasmall nanoparticles has been reported by Capobianco and co-workers.[83] They synthesised $KGdF_4$:Tm^{3+}/Yb^{3+} nanoparticles with size of about ~4 nm by following a co-precipitation approach in OA/ODE. The authors went on to cover the core particles with an inert shell of pure $KGdF_4$ in order to alleviate the surface-related quenching effects. This resulted in an increase in the particle size to 7.4 nm, but also a five-fold improvement in the UC luminescence.[83]

In 2017, Winnik and coworkers further applied the Gd^{3+} doping strategy to prepare $NaLuF_4$-based UCNPs, with particle sizes ranging from 5–15 nm.[84] In this case, the idea was to prepare small UCNPs but with intense upconversion luminescence, visible to the naked eye. To achieve this, the authors

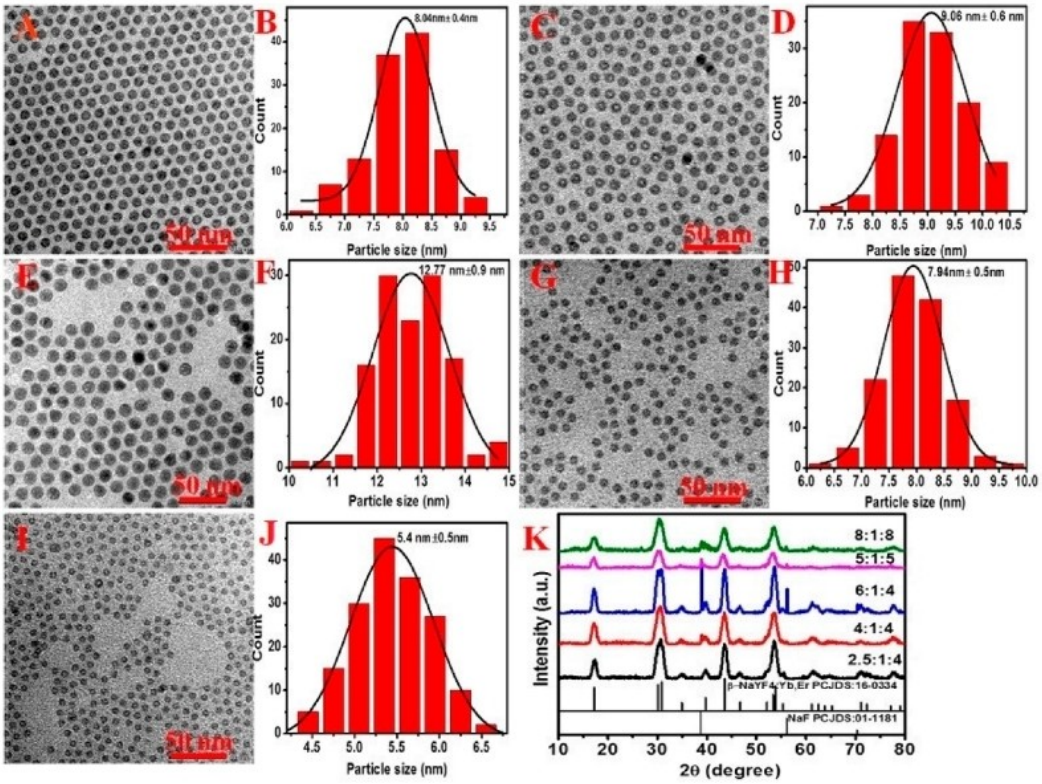

Figure 7. (A–J) Particle size tuning and (K) corresponding phase transition (XRD pattern) in the $NaYF_4$: 30% Yb^{3+}, 2% Er^{3+} UCNPs prepared by Chen and coworkers from different molar ratios of $Ln^{3+}/Na^+/F^-$ (ion ratio used: (A, B) 2.5/1/4, (C, D) 4/1/4, (E, F) 6/1/4, (G, H) 5/1/5, (I, J) 8/1/8). Adapted from ref. [78].

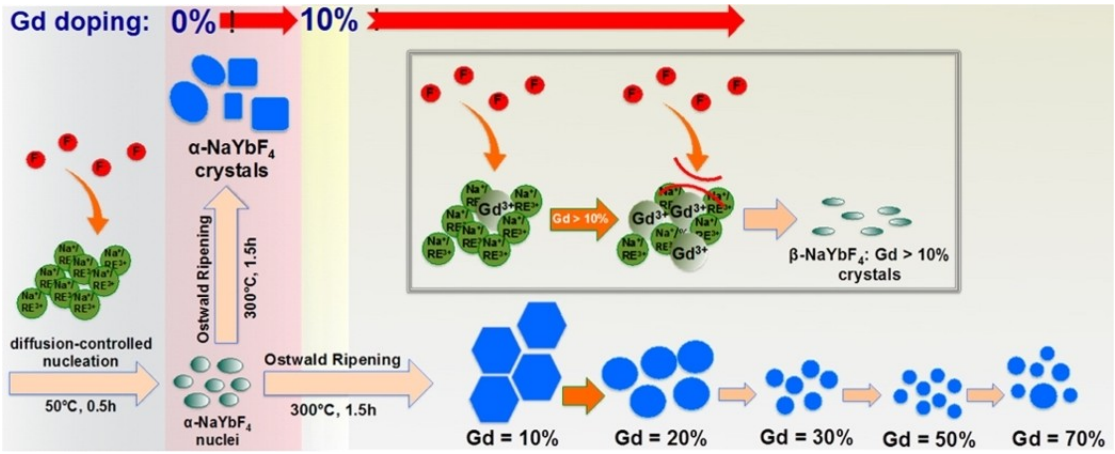

Figure 8. Size and phase tuning of $NaYbF_4$-based nanopsheres realised by Gd^{3+} doping in the crystal lattice. Adapted with permission from ref. [82]. Copyright 2014 American Chemical Society.

used a dopant mixture consisting of Lu (45%), Gd (37%), Yb (16%) and Er (2%). In a one-pot procedure, the Ln salts were heated in a mixture of OA/ODE at 300 °C for 15 min to obtain ~4 nm size nanoparticles.[84] Their synthesis produced the nanoparticles in cubic α-phase, irrespective of the Na/Ln^{3+} and F^-/Ln^{3+} ratios, solvent composition and the reaction temperature employed. Nevertheless, the synthesised $NaLuF_4$:Gd^{3+}/Yb^{3+}/Er^{3+} UCNPs produced intense green emission following excitation with a 978 nm CW laser. The authors noted that changing Lu^{3+} to Y^{3+} ions in the host matrix led to the formation of uniform hexagonal NPs.[84]

Synthesis of sub-10 nm Nd^{3+}-containing UCNPs was reported by Zhang et al.[85] Doping with Nd^{3+} allows for excitation of the UCNPs at 808 nm, which helps to minimise any tissue overheating effects typically associated with 980 nm laser excitation.[85–89] The multilayer nanoparticle architecture consisted of an Yb^{3+}-enriched layer sandwiched in between the $NaGdF_4$:Yb^{3+},Tm^{3+} core and the Nd^{3+}-containing outer shell. Moreover, Ca^{2+} ions were included in the crystal lattice of all layers to limit the luminescence quenching (Figure 9).[85] The nanoparticles were prepared by employing a thermal decomposition route, where the trifluoroacetate precursors were heated in a mixture of OA/ODE at 300 °C, followed by precipitation of the NPs by addition of excess ethanol. All the core, core/shell and core/shell/shell UCNPs were sub-10 nm in size and formed in hexagonal phase, as confirmed by transmission electron microscopy (TEM) and X-ray diffraction (XRD) analysis, respectively.[85] In this synthesis, inclusion of Ca^{2+} ions resulted in a three-fold enhancement of the emission intensity relative to the Ca^{2+} non-doped particles.[85] As a proof-of-concept study, the authors also applied the resulting particles for drug-release under irradiation at a biocompatible wavelength of 808 nm.

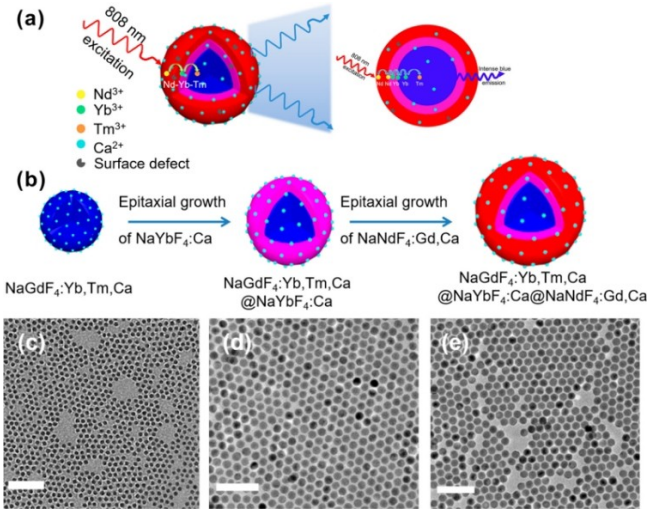

Figure 9. Nd^{3+}-containing ultrasmall UCNPs prepared using a multilayer architecture (TEM scale bar = 50 nm). Adapted with permission from ref. [85]. Copyright 2017 American Chemical Society.

3. Summary and Outlook

This Minireview intends to bring together major synthetic efforts made towards the preparation of ultrasmall UCNPs. Numerous advantages exist for this particular family of NMs in regards to their potential biomedical applications. There has been a significant improvement in understanding the influence of solvent, ion dopants, surface ligands, reaction time and temperature on the growth of UCNPs. This has opened up several possibilities to prepare small-sized UCNPs that also display optical properties tailored for various envisaged applications. However, we are still far behind from delivering such UCNPs into the clinics. For example, full control over the toxicological effects of UCNPs or their stability in a biochemical environment is still lacking.[28,30,41,51–52] As for the other NMs, making renal clearable UCNPs can be foreseen as a way to limit any potential toxic effects. However, this requires reducing their

size to below 10 nm, which in turn leads to decreased emission intensity. Using organic dyes to sensitise the UC has been proposed as one alternate way to compensate for the encountered loss in UC intensity due to the size reduction.[4] In other developments, new surface modification strategies that can help to minimise the quenching effects, enhance the in vivo stability of UCNPs and make them resistant to non-specific interaction with proteins are being pursued with great interest. Some of the synthesis' summarised in this minireview present a good starting point to implement these modification protocols in order to generate UCNPs that can ultimately be translated into clinics as diagnostic and therapeutic probes. From this perspective, it is a highly encouraging sign that researchers are now pushing more towards establishing collaborative networks for up-scaled material synthesis', surface modifications, photophysical characterisations, and toxicological evaluations to be able to accelerate the progress in this direction.[10,90]

Acknowledgements

This work was supported by the Helmholtz Initiative and Networking Fund (Functional Nanomaterials for Multimodality Cancer Imaging (NanoTracking), project ID: VH-VI-421), and an Alexander von Humboldt Foundation research fellowship to T.J.

Conflict of Interest

The authors declare no conflict of interest.

Keywords: lanthanides · nanomaterials · photophysical properties · ultrasmall size · upconversion

[1] S. Wilhelm, M. Kaiser, C. Wurth, J. Heiland, C. Carrillo-Carrion, V. Muhr, O. S. Wolfbeis, W. J. Parak, U. Resch-Genger, T. Hirsch, *Nanoscale* **2015**, *7*, 1403–1410.
[2] X. Liu, C.-H. Yan, J. A. Capobianco, *Chem. Soc. Rev.* **2015**, *44*, 1299–1301.
[3] M. Haase, H. Schafer, *Angew. Chem. Int. Ed.* **2011**, *50*, 5808–5829; *Angew. Chem.* **2011**, *123*, 5928–5950.
[4] S. Wen, J. Zhou, K. Zheng, A. Bednarkiewicz, X. Liu, D. Jin, *Nat. Commun.* **2018**, *9*, 2415.
[5] A. Gulzar, J. T. Xu, P. P. Yang, F. He, L. G. Xu, *Nanoscale* **2017**, *9*, 12248–12282.
[6] V. Marturano, J. Kozlowska, A. Bajek, M. Giamberini, V. Ambrogi, P. Cerruti, R. Garcia-Valls, J. M. Montornes, B. Tylkowski, *Coord. Chem. Rev.* **2019**, *398*, 213013.
[7] G. Jalani, V. Tam, F. Vetrone, M. Cerruti, *J. Am. Chem. Soc.* **2018**, *140*, 10923–10931.
[8] X. J. Zhu, Q. Q. Su, W. Feng, F. Y. Li, *Chem. Soc. Rev.* **2017**, *46*, 1025–1039.
[9] S. Wu, J. P. Blinco, C. Barner-Kowollik, *Chem. Eur. J.* **2017**, *23*, 8325–8332.
[10] S. Wilhelm, *ACS Nano* **2017**, *11*, 10644–10653.
[11] H. Dong, S. R. Du, X. Y. Zheng, G. M. Lyu, L. D. Sun, L. D. Li, P. Z. Zhang, C. Zhang, C. H. Yan, *Chem. Rev.* **2015**, *115*, 10725–10815.
[12] G. Chen, H. Ågren, T. Y. Ohulchanskyy, P. N. Prasad, *Chem. Soc. Rev.* **2015**, *44*, 1680–1713.
[13] S. Wu, H.-J. Butt, *Adv. Mater.* **2016**, *28*, 1208–1226.
[14] Y. I. Park, K. T. Lee, Y. D. Suh, T. Hyeon, *Chem. Soc. Rev.* **2015**, *44*, 1302–1317.
[15] J.-C. G. Bunzli, S. V. Eliseeva, *Chem. Sci.* **2013**, *4*, 1939–1949.
[16] H. Dong, L.-D. Sun, C.-H. Yan, *Chem. Soc. Rev.* **2015**, *44*, 1608–1634.
[17] X. Chen, D. Peng, Q. Ju, F. Wang, *Chem. Soc. Rev.* **2015**, *44*, 1318–1330.
[18] E. M. Chan, E. S. Levy, B. E. Cohen, *Adv. Mater.* **2015**, *27*, 5753–5761.
[19] E. Blanco, H. Shen, M. Ferrari, *Nat. Biotechnol.* **2015**, *33*, 941–951.
[20] L.-D. Sun, Y.-F. Wang, C.-H. Yan, *Acc. Chem. Res.* **2014**, *47*, 1001–1009.
[21] V. Muhr, S. Wilhelm, T. Hirsch, O. S. Wolfbeis, *Acc. Chem. Res.* **2014**, *47*, 3481–3493.
[22] J. Zhou, Z. Liu, F. Li, *Chem. Soc. Rev.* **2012**, *41*, 1323–1349.
[23] Z. J. Gu, L. Yan, G. Tian, S. J. Li, Z. F. Chai, Y. L. Zhao, *Adv. Mater.* **2013**, *25*, 3758–3779.
[24] J. Nam, N. Won, J. Bang, H. Jin, J. Park, S. Jung, S. Jung, Y. Park, S. Kim, *Adv. Drug Delivery Rev.* **2013**, *65*, 622–648.
[25] G. Chen, H. Qiu, P. N. Prasad, X. Chen, *Chem. Rev.* **2014**, *114*, 5161–5214.
[26] H. Dong, S.-R. Du, X.-Y. Zheng, G.-M. Lyu, L.-D. Sun, L.-D. Li, P.-Z. Zhang, C. Zhang, C.-H. Yan, *Chem. Rev.* **2015**, *115*, 10725–10815.
[27] A. Escudero, C. Carrillo-Carrión, M. V. Zyuzin, W. J. Parak, *Top. Curr. Chem.* **2016**, *374*, 48.
[28] A. Gulzar, J. Xu, P. Yang, F. He, L. Xu, *Nanoscale* **2017**, *9*, 12248–12282.
[29] A. Sedlmeier, H. H. Gorris, *Chem. Soc. Rev.* **2015**, *44*, 1526–1560.
[30] S. Roy, Z. Liu, X. Sun, M. Gharib, H. Yan, Y. Huang, S. Megahed, M. Schnabel, D. Zhu, N. Feliu, I. Chakraborty, C. Sanchez-Cano, A. M. Alkilany, W. J. Parak, *Bioconjugate Chem.* **2019**, *30*, 2751–2762.
[31] T. L. Moore, L. Rodriguez-Lorenzo, V. Hirsch, S. Balog, D. Urban, C. Jud, B. Rothen-Rutishauser, M. Lattuada, A. Petri-Fink, *Chem. Soc. Rev.* **2015**, *44*, 6287–6305.
[32] S. J. Soenen, W. J. Parak, J. Rejman, B. Manshian, *Chem. Rev.* **2015**, *115*, 2109–2135.
[33] O. Plohl, S. Kralj, B. Majaron, E. Fröhlich, M. Ponikvar-Svet, D. Makovec, D. Lisjak, *Dalton Trans.* **2017**, *46*, 6975–6984.
[34] A. Aebischer, S. Heer, D. Biner, K. Krämer, M. Haase, H. U. Güdel, *Chem. Phys. Lett.* **2005**, *407*, 124–128.
[35] X. Li, F. Zhang, D. Zhao, *Chem. Soc. Rev.* **2015**, *44*, 1346–1378.
[36] S. Gai, C. Li, P. Yang, J. Lin, *Chem. Rev.* **2014**, *114*, 2343–2389.
[37] G. Tessitore, S. L. Maurizio, T. Sabri, J. A. Capobianco, *Angew. Chem. Int. Ed.* **2019**, *58*, 9742–9751.
[38] J. Zuo, Q. Li, B. Xue, C. Li, Y. Chang, Y. Zhang, X. Liu, L. Tu, H. Zhang, X. Kong, *Nanoscale* **2017**, *9*, 7941–7946.
[39] U. Resch-Genger, H. H. Gorris, *Anal. Bioanal. Chem.* **2017**, *409*, 5855–5874.
[40] B. Zhou, B. Shi, D. Jin, X. Liu, *Nat. Nanotechnol.* **2015**, *10*, 924–936.
[41] Y. Zhang, Y. Bai, J. Jia, N. Gao, Y. Li, R. Zhang, G. Jiang, B. Yan, *Chem. Soc. Rev.* **2014**, *43*, 3762–3809.
[42] Y. K. Lee, E. J. Choi, T. J. Webster, S. H. Kim, D. Khang, *Int. J. Nanomed.* **2015**, *10*, 97–112.
[43] K. Zarschler, L. Rocks, N. Licciardello, L. Boselli, E. Polo, K. P. Garcia, L. De Cola, H. Stephan, K. A. Dawson, *Nanomedicine* **2016**, *12*, 1663–1701.
[44] C. Li, L. Xu, Z. Liu, Z. Li, Z. Quan, A. A. Al Kheraif, J. Lin, *Dalton Trans.* **2018**, *47*, 8538–8556.
[45] K. P. García, K. Zarschler, L. Barbaro, J. A. Barreto, W. O'Malley, L. Spiccia, H. Stephan, B. Graham, *Small* **2014**, *10*, 2516–2529.
[46] Y. Wei, L. Quan, C. Zhou, Q. Zhan, *Nanomedicine* **2018**, *13*, 1495–1512.
[47] P. Foroozandeh, A. A. Aziz, *Nanoscale Res. Lett.* **2015**, *10*, 221.
[48] N. Feliu, D. Docter, M. Heine, P. Del Pino, S. Ashraf, J. Kolosnjaj-Tabi, P. Macchiarini, P. Nielsen, D. Alloyeau, F. Gazeau, R. H. Stauber, W. J. Parak, *Chem. Soc. Rev.* **2016**, *45*, 2440–2457.
[49] A. Nsubuga, M. Sgarzi, K. Zarschler, M. Kubeil, R. Hübner, R. Steudtner, B. Graham, T. Joshi, H. Stephan, *Dalton Trans.* **2018**, *47*, 8595–8604.
[50] A. Nsubuga, K. Zarschler, M. Sgarzi, B. Graham, H. Stephan, T. Joshi, *Angew. Chem. Int. Ed.* **2018**, *57*, 16036–16040.
[51] A. Gnach, T. Lipinski, A. Bednarkiewicz, J. Rybka, J. A. Capobianco, *Chem. Soc. Rev.* **2015**, *44*, 1561–1584.
[52] Y. Sun, W. Feng, P. Yang, C. Huang, F. Li, *Chem. Soc. Rev.* **2015**, *44*, 1509–1525.
[53] J. Zhao, Z. Lu, Y. Yin, C. McRae, J. A. Piper, J. M. Dawes, D. Jin, E. M. Goldys, *Nanoscale* **2013**, *5*, 944–952.
[54] B. Chen, F. Wang, *Acc. Chem. Res.* **2020**, *53*, 358–367.
[55] D. Hudry, I. A. Howard, R. Popescu, D. Gerthsen, B. S. Richards, *Adv. Mater.* **2019**, *31*, 1900623.
[56] S. F. Himmelstoß, T. Hirsch, *Methods Appl. Fluoresc.* **2019**, *7*, 022002.
[57] E. Andresen, U. Resch-Genger, M. Schäferling, *Langmuir* **2019**, *35*, 5093–5113.
[58] R. Naccache, Q. Yu, J. A. Capobianco, *Adv. Opt. Mater.* **2015**, *3*, 482–509.
[59] F. Wang, X. Liu, *Acc. Chem. Res.* **2014**, *47*, 1378–1385.
[60] S. Radunz, A. Schavkan, S. Wahl, C. Würth, H. R. Tschiche, M. Krumrey, U. Resch-Genger, *J. Phys. Chem. C* **2018**, *122*, 28958–28967.

[61] A. Escudero, A. I. Becerro, C. Carrillo-Carrión, N. O. Núñez, M. V. Zyuzin, M. Laguna, D. González-Mancebo, M. Ocaña, W. J. Parak, *Nat. Photonics* **2017**, *6*, 881.
[62] S. N. Achary, S. Bevara, A. K. Tyagi, *Coord. Chem. Rev.* **2017**, *340*, 266–297.
[63] C. Homann, J. Bolze, M. Haase, *Part. Part. Syst. Charact.* **2019**, *36*, 1800391.
[64] Y. Liu, D. Tu, H. Zhu, X. Chen, *Chem. Soc. Rev.* **2013**, *42*, 6924–6958.
[65] A. Gnach, A. Bednarkiewicz, *Nano Today* **2012**, *7*, 532–563.
[66] C. Yan, H. Zhao, D. F. Perepichka, F. Rosei, *Small* **2016**, *12*, 3888–3907.
[67] W. Niu, S. Wu, S. Zhang, *J. Mater. Chem.* **2011**, *21*, 10894–10902.
[68] G. Chen, T. Y. Ohulchanskyy, R. Kumar, H. Ågren, P. N. Prasad, *ACS Nano* **2010**, *4*, 3163–3168.
[69] X. Zhai, S. Liu, Y. Zhang, G. Qin, W. Qin, *J. Mater. Chem. C* **2014**, *2*, 2037–2044.
[70] A. D. Ostrowski, E. M. Chan, D. J. Gargas, E. M. Katz, G. Han, P. J. Schuck, D. J. Milliron, B. E. Cohen, *ACS Nano* **2012**, *6*, 2686–2692.
[71] J. Shan, X. Qin, N. Yao, Y. Ju, *Nanotechnology* **2007**, *18*.
[72] J. Hesse, D. T. Klier, M. Sgarzi, A. Nsubuga, C. Bauer, J. Grenzer, R. Hübner, M. Wislicenus, T. Joshi, M. U. Kumke, H. Stephan, *ChemistryOpen* **2018**, *7*, 159–168.
[73] S. Dühnen, T. Rinkel, M. Haase, *Chem. Mater.* **2015**, *27*, 4033–4039.
[74] T. Rinkel, J. Nordmann, A. N. Raj, M. Haase, *Nanoscale* **2014**, *6*, 14523–14530.
[75] T. Rinkel, A. N. Raj, S. Dühnen, M. Haase, *Angew. Chem. Int. Ed.* **2016**, *55*, 1164–1167; *Angew. Chem.* **2016**, *128*, 1177–1181.
[76] R. Shi, X. Ling, X. Li, L. Zhang, M. Lu, X. Xie, L. Huang, W. Huang, *Nanoscale* **2017**, *9*, 13739–13746.
[77] H.-X. Mai, Y.-W. Zhang, R. Si, Z.-G. Yan, L.-d. Sun, L.-P. You, C.-H. Yan, *J. Am. Chem. Soc.* **2006**, *128*, 6426–6436.
[78] H. Li, L. Xu, G. Chen, *Molecules* **2017**, *22*, 2113.
[79] F. Wang, Y. Han, C. S. Lim, Y. Lu, J. Wang, J. Xu, H. Chen, C. Zhang, M. Hong, X. Liu, *Nature* **2010**, *463*, 1061–1065.
[80] A. Skripka, R. Marin, A. Benayas, P. Canton, E. Hemmer, F. Vetrone, *Phys. Chem. Chem. Phys.* **2017**, *19*, 11825–11834.
[81] Q. Liu, Y. Sun, T. Yang, W. Feng, C. Li, F. Li, *J. Am. Chem. Soc.* **2011**, *133*, 17122–17125.
[82] J. A. Damasco, G. Chen, W. Shao, H. Ågren, H. Huang, W. Song, J. F. Lovell, P. N. Prasad, *ACS Appl. Mater. Interfaces* **2014**, *6*, 13884–13893.
[83] H.-T. Wong, F. Vetrone, R. Naccache, H. L. W. Chan, J. Hao, J. A. Capobianco, *J. Mater. Chem.* **2011**, *21*, 16589–16596.
[84] E. Lu, J. Pichaandi, L. P. Arnett, L. Tong, M. A. Winnik, *J. Phys. Chem. C* **2017**, *121*, 18178–18185.
[85] Y. Zhang, Z. Yu, J. Li, Y. Ao, J. Xue, Z. Zeng, X. Yang, T. T. Y. Tan, *ACS Nano* **2017**, *11*, 2846–2857.
[86] Y. F. Wang, G. Y. Liu, L. D. Sun, J. W. Xiao, J. C. Zhou, C. H. Yan, *ACS Nano* **2013**, *7*, 7200–7206.
[87] M.-H. Chan, R.-S. Liu, *Nanoscale* **2017**, *9*, 18153–18168.
[88] S. Hao, G. Chen, C. Yang, W. Shao, W. Wei, Y. Liu, P. N. Prasad, *Nanoscale* **2017**, *9*, 10633–10638.
[89] X. Huang, J. Lin, *J. Mater. Chem. C* **2015**, *3*, 7652–7657.
[90] H. Oliveira, A. Bednarkiewicz, A. Falk, E. Fröhlich, D. Lisjak, A. Prina-Mello, S. Resch, C. Schimpel, I. V. Vrček, E. Wysokińska, H. H. Gorris, *Adv. Healthcare Mater.* **2019**, *8*, 1801233.

Manuscript received: March 17, 2020
Revised manuscript received: May 25, 2020